JOURNAL OF Materials CHEMISTRY

Synthesis, structural characterization, thermal stability and electrical properties of the new phases $M^{I}Ga(CrO_4)_2$ (M^{I} = Na, K, Rb)

M. Jesus Saavedra,[a] Carmen Parada[a] and Jose M. Rojo[b]

[a]*Departamento de Química Inorgánica, Facultad de Ciencias Químicas, Universidad Complutense, 28040 Madrid, Spain*

[b]*Instituto Ciencia de Materiales de Madrid, CSIC, Cantoblanco, 28049 Madrid, Spain*

New phases of composition $M^{I}Ga(CrO_4)_2$ (M^{I} = Na, K or Rb) have been synthesized by solid state reaction in air. The crystallograhic data of the three compounds have been refined by the Rietveld method. They all show a layer structure, the layer being formed of GaO_6 octahedra linked to CrO_4 tetrahedra by sharing corners. Alkali metal ions lie in the interlayer space. The three compounds are thermally stable up to 300 °C, but above this temperature they decompose evolving oxygen. Impedance measurements show that they are ion conductors, the ionic conductivity being highest for the Na compound.

Introduction

There are many phases with the stoichiometry $M^{I}M^{III}(XO_4)_2$ in which M^{I} is an alkali metal ion, NH_4^+ or Tl^+, M^{III} is a transition metal, and X is an element that forms a tetrahedral oxoanion such as S, Cr or Mo. These phases crystallize with different structural types depending on the size of the monovalent cation. In the case of phases with formula $M^{I}M^{III}(CrO_4)_2$, there are three different structural types as follows.

(i) When M^{I} is Li, the phase $LiM^{III}(CrO_4)_2$ where M^{III} = Fe or Cr crystallizes in a three-dimensional structure with orthorhombic symmetry in the space group *Cmcm*,[1,2] being isostructural with $CrVO_4$.[3–7]

(ii) When the alkali metals are of intermediate size (M^{I} = Na, K or Rb) the phases $M^{I}M^{III}(CrO_4)_2$ where M^{III} = Al, Fe or Cr show a layered structure with monoclinic symmetry in the space group *C*2/*m*.[8–10]

(iii) When M^{I} is Cs, the structure is also layered, but the symmetry is orthorhombic and the space group is *Pnma*. This structure, which is similar to that of the second class, shows a different orientation of the polyhedra and a different stacking sequence of the layers.[2,11,12]

The structure of the second type of compounds is very similar to the mineral yavapaiite and can be described in two different ways.[13,14] One way is to describe the structure as formed of layers which are built up of $M^{III}O_6$ octahedra and CrO_4 tetrahedra linked together by vertices so that each octahedron is linked to six tetrahedra and each tetrahedron is linked to three octahedra. The fourth vertex of each tetrahedon remains unshared and points into the interlayer space. The negative charge of the layers is compensated by alkali metal cations which are located at the interlayer space[15] (Fig. 1). Another way of describing the structure is as a hexagonal closed-packed arrangement of $(CrO_4)^{2-}$ in which all the octahedral sites are occupied by M^{III} and these alternate with layers of M^+ cations.[16]

The purpose of this work is the synthesis of new compounds of composition $M^{I}Ga(CrO_4)_2$ (M^{I} = Na, K or Rb), all belonging to the second structural type. A study of the ionic conductivity of these phases has also been undertaken.

Experimental

Phases of composition $M^{I}Ga(CrO_4)_2$ (M^{I} = Na, K or Rb) were obtained by solid state reaction from stoichiometric mixtures of the reagents $Ga(NO_3)_3{\cdot}9H_2O$, CrO_3 and $M^{I}NO_3$ in the molar ratio 1:2:1. The mixtures were heated at increasing temperature as follows: 100 °C for 24 h, 200 °C for 24 h, and 300 °C for 192 h. After these treatements very pure and well crystallized powder samples were obtained. The three compounds exhibited a similar green–black colour.

X-Ray diffraction patterns were recorded on a SIEMENS D-500 diffractometer using Cu-Kα radiation [λ = 1.540 981 Å]. The scan was carried out in steps of 0.04°, counting for 24 s at each step between 5 and 70 2θ. The X-ray diffraction data were analyzed by the Rietveld method[17,18] using the FULLPROF program.[19]

Thermal decomposition of the samples was followed in a METTLER thermobalance (model T.G.50). The experiments was conducted with the samples under an N_2 flow at a heating rate of 10 °C min^{-1}.

Electrical measurements were carried out by the complex impedance method by using a 1174 SOLARTRON frequency response analyzer. Parallelepiped pellets with dimensions (10 × 2.5 × 2.5 mm) were previously sintered in a furnace at 300 °C for 24 hours. Gold electrodes were deposited on two opposite faces of the pellets by vacuum evaporation. The frequency range employed was 10^{-1}–10^5 Hz. The measurements were carried out at different temperatures in the range 40–320 °C, with the pellet under a dried N_2 flow. In the heating and cooling runs the temperature increment was 20 °C, and before each measurement the samples were kept at the indicated

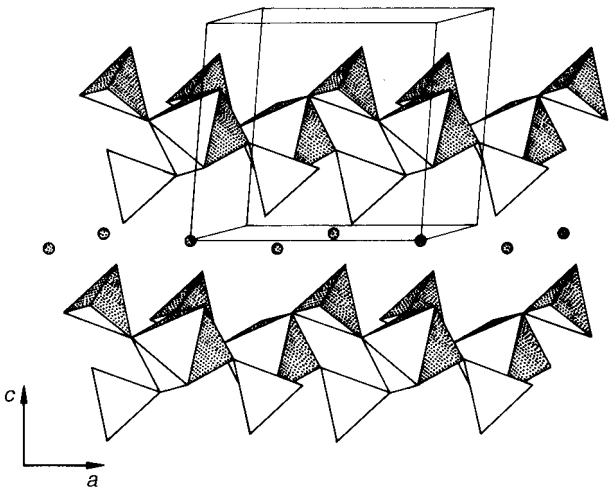

Fig. 1 Crystal structure of $KCr(CrO_4)_2$.

temperature for 20 min. The density of the pellets was determined by immersion in ethanol according to the Archimedes method.

Results and discussion

Crystallographic data

The X-ray powder data show that this new series of compounds is isostructural to $M^{I}Cr(CrO_4)_2$ (M^{I}=Na, K or Rb).[8] The structure of the three new compounds $NaGa(CrO_4)_2$, $KGa(CrO_4)_2$ and $RbGa(CrO_4)_2$ was refined using the Rietveld technique.[17,18] The obtained crystallographic data as well as the conditions of the diffraction experiments for the three compounds are summarized in Table 1. The observed and calculated X-ray diffraction patterns are shown in Fig. 2. The atomic coordinates for the $KCr(CrO_4)_2$ structure [8] were used as the starting coordinates. Rietveld refinement was made using the FULLPROF program.[18] The final values of the atomic coordinates and thermal parameters are listed in Table 2 and interatomic distances are listed in Table 3.

The structure of $KCr(CrO_4)_2$ is shown in Fig. 1. The gallium atoms are located in the $[Ga(CrO_4)_2]_n^{n-}$ layers in which $Ga^{III}O_6$ octahedra and $Cr^{VI}O_4$ tetrahedra are linked by sharing corners. Each gallium atom is coordinated by four O3 and two O1 atoms, while the chromium atom is coordinated by two O3, and one O1 atom. The fourth oxygen atom, O2, is unshared and pointing to the interlayer space. The alkali metal cations (Na, K, Rb) which lie in between layers are surrounded by ten oxygen atoms: two O2, four O3 and another four O2 at an increased separation. The alkali metal–oxygen distances are listed in Table 3.

Thermal decomposition

The thermal decomposition is the same for all compounds and can be expressed by eqn. (1)

$$M^{I}Ga(CrO_4)_2 \rightarrow 0.5M^{I}_2CrO_4 + 0.75Cr_2O_3 + 0.5Ga_2O_3 + 1.125O_2\uparrow \quad (1)$$

X-Ray powder patterns confirmed the presence of these compounds and Table 4 lists the temperature ranges in which the decomposition occurred as well as the observed and calculated weight losses. The experimental weight loss, which is due to the release of oxygen, is also in good agreement with the proposed reaction.

Table 1 Crystallographic data, recording conditions and refinement results of $M^{I}Ga(CrO_4)_2$ (M^{I}=Na, K, Rb)

	$NaGa(CrO_4)_2$	$KGa(CrO_4)_2$	$RbGa(CrO_4)_2$
space group	*C*2/*m*	*C*2/*m*	*C*2/*m*
2θ range/°	5–70	5–70	5–70
step scan increment (2θ/°)	0.04	0.04	0.04
unit-cell parameters			
a/Å	8.4922(7)	8.5700(1)	8.5974(7)
b/Å	5.4708(4)	5.4612(3)	5.4576(4)
c/Å	6.8051(5)	7.6343(7)	7.9595(7)
β/°	91.334(4)	95.184(6)	95.927(6)
V/Å^3	316.07	355.84	371.47
Z	2	2	2
profile parameters			
U	0.3303	0.48603	0.30811
V	−0.14730	−0.16551	−0.12187
W	0.05398	0.06060	0.05227
reliance factors[a]	11.1	9.57	10.4
R_{WP}	8.84	7.56	8.02
R_P	7.6	8.3	9
R_B	3.92	3.09	2.95

[a]Defined as follows: $R_{WP}=[\Sigma w_i[Y_{obs}-Y_{calc}]^2/\Sigma w_i[Y_{obs}]^{1/2}]$, $R_P=(\Sigma |Y_{obs}-Y_{calc}|)/(\Sigma Y_{obs})$, $R_B=(100\Sigma |I_{obs}-I_{cal}|)/(\Sigma I_{obs})$.

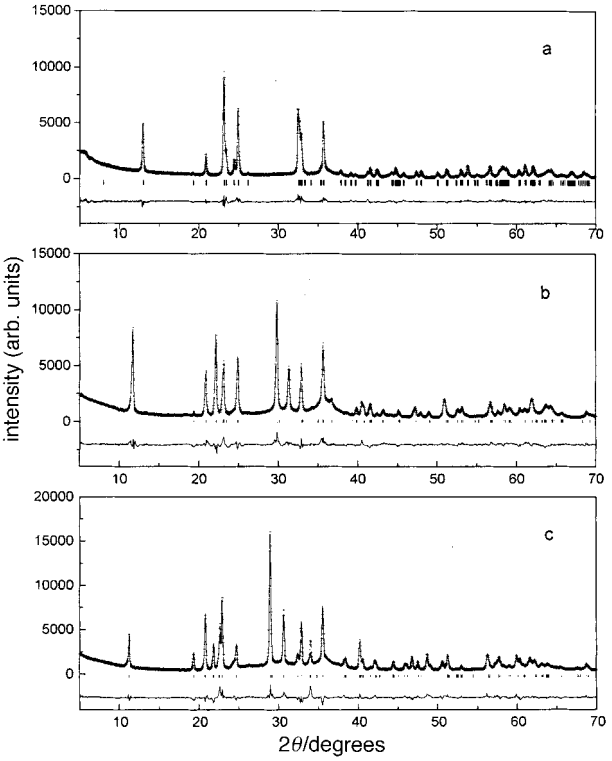

Fig. 2 Experimental (+) and calculated (solid line) X-ray diffraction patterns for (a) $NaGa(CrO_4)_2$, (b) $KGa(CrO_4)_2$ and (c) $RbGa(CrO_4)_2$. The difference between experimental and calculated data is plotted at the bottom. Vertical marks indicate the position of the allowed Bragg reflections.

Table 2 Fractional atomic coordinates for $M^{I}Ga(CrO_4)_2$ (M^{I}=Na, K or Rb)[a]

compound	atom	*x*	*y*	*z*
$NaGa(CrO_4)_2$	Na	0.0	0.0	0.0
	Ga	0.0	0.0	0.5
	Cr	0.6631(4)	0.0	0.2737(7)
	O1	0.2293(5)	0.0	0.5594(7)
	O2	0.7095(6)	0.0	0.0564(6)
	O3	0.0285(8)	0.2479(8)	0.2853(8)
$KGa(CrO_4)_2$	K	0.0	0.0	0.0
	Ga	0.0	0.0	0.5
	Cr	0.6251(6)	0.0	0.2932(5)
	O1	0.2293(9)	0.0	0.5595(7)
	O2	0.6951(8)	0.0	0.0951(8)
	O3	0.0182(7)	0.2567(7)	0.3087(9)
$RbGa(CrO_4)_2$	Rb	0.0	0.0	0.0
	Ga	0.0	0.0	0.5
	Cr	0.6286(5)	0.0	0.3032(6)
	O1	0.2232(7)	0.0	0.5557(8)
	O2	0.6834(5)	0.0	0.1103(7)
	O3	0.0120(8)	0.2722(6)	0.3194(9)

[a]Overall isotropic thermal parameter = 1.07(3) Å^2 for $NaGa(CrO_4)_2$, 1.53(5) Å^2 for $KGa(CrO_4)_2$ and 2.18(1) Å^2 for $RbGa(CrO_4)_2$.

Ionic conductivity

The impedance plots ($-Z''$ *vs.* $-Z'$) of a $NaGa(CrO_4)_2$ pellet recorded at two temperatures are shown in Fig. 3 (top). At low temperatures (180 °C) an arc is observed. When the temperature is raised (300 °C) the arc disappears and an inclined spike is detected. A similar behavior is observed for $KGa(CrO_4)_2$ and $RbGa(CrO_4)_2$ pellets. In all cases the spike is due to the blocking effect of the alkali metal ions at the electrode surfaces while the arc gives information of the dielectric behavior of the pellets. The capacitance of the arc is in the range 2–5 pF for all the pellets. The resistance was determined from the intercept of the low-frequency end of the

Table 3 Interatomic distances (Å) in $M^{I}Ga(CrO_4)_2$ (M^{I}=Na, K or Rb)

distance/Å	$NaGa(CrO_4)_2$	$KGa(CrO_4)_2$	$RbGa(CrO_4)_2$
$M^{I}-M^{I}$ (×4)	5.051(3)	5.081(2)	5.092(3)
$M^{I}-Ga$ (×2)	3.402(2)	3.817(4)	3.987(5)
$M^{I}-Cr$ (×4)	3.483(3)	3.629(5)	3.734(4)
$M^{I}-O2$ (×2)	2.505(5)	2.774(2)	2.945(3)
$M^{I}-O2$ (×4)	3.281(3)	3.249(3)	3.228(3)
$M^{I}-O3$ (×4)	2.376(2)	2.734(4)	2.937(4)
Ga−O1 (×2)	1.979(4)	1.976(5)	1.924(6)
Ga−O3 (×4)	2.012(6)	2.040(4)	2.077(4)
Cr−O1	1.610(2)	1.604(3)	1.609(5)
Cr−O2	1.626(3)	1.674(5)	1.652(5)
Cr−O3 (×2)	1.643(5)	1.625(4)	1.610(6)
O1−O1(×2)	2.876(6)	2.909(5)	2.920(6)
O2−O2 (×2)	2.927(7)	3.271(6)	3.501(7)
O3−O3	2.712(5)	2.657(8)	2.486(5)
O3−O3	2.758(7)	2.804(6)	2.903(8)
O3−O3	2.973(5)	2.965(6)	2.971(5)

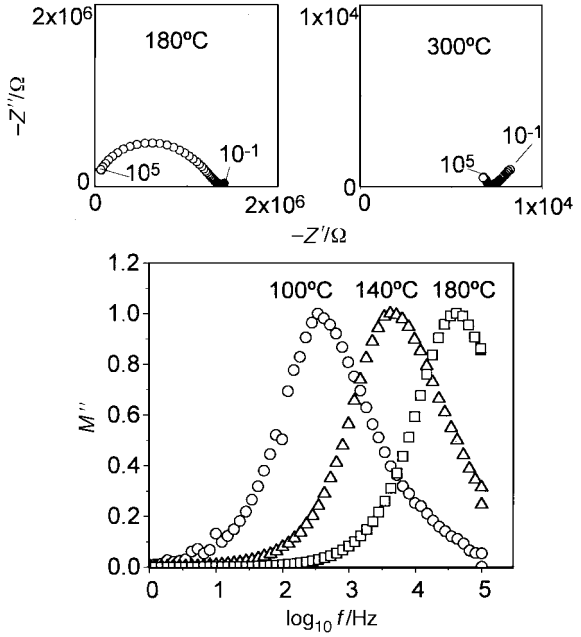

Fig. 3 Top: impedance plots recorded at two temperatures for the $NaGa(CrO_4)_2$ pellet. The data were obtained in the frequency range 10^{-1}–10^5 Hz. The best fit (◇) to the arc (○) is obtained according to the expression $1/Z^*=1/R+B(i\omega)^n+i\omega C$; parameters are $R=7.5\times10^5$ Ω, $B(CPE)=1.9\times10^{-9}$, $n(CPE)=0.55$ and $C=2\times10^{-12}$F. Bottom: normalized imaginary part of the electric modulus *vs.* frequency at the indicated temperatures.

Table 4 Temperature ranges, observed and calculated weight, of the thermal decomposition

sample	temperature range	Δm_{obs} (%)	Δm_{calc} (%)
$NaGa(CrO_4)_2$	350–620 °C	10.97	11.08
$KGa(CrO_4)_2$	325–615 °C	10.34	10.56
$RbGa(CrO_4)_2$	315–610 °C	9.18	9.29

arc on the real Z' axis and the conductivity was calculated as usual. The resistance determined by this way is in agreement with that deduced from the fit of the arc to the expression $1/Z^*=1/R+B(i\omega)^n+i\omega C$, where the first term accounts for the resistance, the second for a CPE element, and the third for the capacitance whose contribution becomes more significant as the frequency increases. The expression corresponds to a parallel circuit of the three elements already mentioned. Diamonds in the impedance plot at 180 °C (Fig. 3, top) show the best fit to the experimental arc.

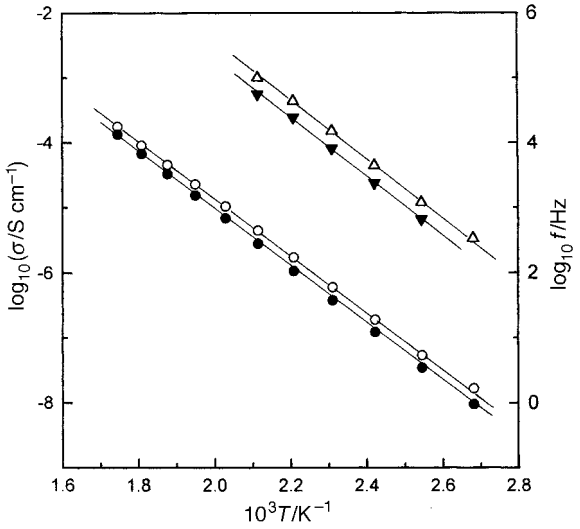

Fig. 4 Arrhenius plots for conductivity (circles) and frequency (triangles). Open and closed symbols correspond to the data obtained for the Na pellet with the electric field perpendicular and parallel to the compaction force, respectively.

The imaginary part of the dielectric modulus (M''), related to the impedance through the expression $M''\omega \propto Z'$, where f and Z' are the frequency and the real part of the impedance, respectively, is often used because this parameter gives information on the grain–interior response but it is not affected by grain-boundary and electrode effects.[20–22] The normalized M'' *vs.* f at different temperatures is plotted in a semilog scale in Fig. 3 (bottom). An asymmetric peak is observed which shifts towards high frequency with increasing temperature.

Taking into account the layer structure of the $M^{I}Ga(CrO_4)_2$ (M^{I}=Na, K or Rb) compounds, particles of the powder samples could adopt a preferential orientation when they are compacted under pressure to form pellets. Thus electrical measurements were carried out by applying the electric field in two directions: one, in the same direction as the force used in the compaction and the other in a direction perpendicular to that force. The temperature dependence of the conductivity in the two directions for the $NaGa(CrO_4)_2$ pellet is shown in Fig. 4. The frequency measured at the maximum of the M'' peak is also included for the two directions in the same figure (Fig. 4). The conductivity and frequency data are well fitted to the expressions $\sigma=\sigma_0\exp(-E_\sigma/kT)$ and $f=f_0\exp(-E_f/kT)$, where σ_0 and f_0 are pre-exponential factors, E_σ and E_f activation energies, and k the Boltzmann constant. The values of the pre-exponential factors and activation energies corresponding to the best fits together with the conductivity measured at 180 °C are shown in Table 5. It is observed that E_σ and E_f coincide within experimental error (0.02 eV) indicating that the impedance arc shown in Fig. 3 is dominated by the grain–interior response. This result is consistent with the high density of the pellets, the relative density being 86, 93 and 97% for the Na, K, and Rb pellet, respectively. The conductivity measured in the two directions is similar indicating that the particles are not preferentially oriented according to the layer structure.

A comparative study between $NaGa(CrO_4)_2$, $KGa(CrO_4)_2$ and $RbGa(CrO_4)_2$ has been made. The temperature dependence of the conductivity is shown in Fig. 5. In spite of the fact that a preferential orientation was not observed, the conductivity was measured in all three cases on pellets in which the electric field was applied in a direction perpendicular to that of the force used during compaction. The data are well fitted to the Arrhenius expression already mentioned and the activation energy (E_σ) and pre-exponential factor (σ_o) are listed

Table 5 Activation energies (E_σ and E_f) and pre-exponential factors (σ_0 and f_0) for the Arrhenius plots of Fig. 4. Conductivity at 180 °C is also included

sample	E_σ/eV	$10^{-3}\ \sigma_0$/S cm^{-1}	$10^{6}\ \sigma$(180 °C)/S cm^{-1}	E_f/eV	$10^{-14}\ f_0$/Hz
$NaGa(CrO_4)_2$ ($\perp$)	0.86	6.6	1.9	0.88	2.5
$NaGa(CrO_4)_2$ ($\parallel$)	0.88	7.3	1.2	0.90	2.3

Table 6 Activation energy (E_a) and pre-exponential factor(σ_0) for the Arrhenius plots of Fig. 5. Conductivity at 180 °C is included for comparison

sample	E_σ/eV	σ_0/S cm^{-1}	σ (180 °C)/S cm^{-1}
$NaGa(CrO_4)_2$	0.86	6.6×10^{3}	1.9×10^{6}
$KGa(CrO_4)_2$	1.25	4.9×10^{6}	4.5×10^{8}
$RbGa(CrO_4)_2$	1.38	7.6×10^{7}	3.0×10^{-8}

Table 7 Alkali metal diameters (r), distances O2···O2(d) and ratios d/r

cation	r/Å	d/Å	d/r
Na	2.58	2.927 (7)	1.13
K	3.18	3.271 (6)	1.03
Rb	3.32	3.501 (7)	1.05

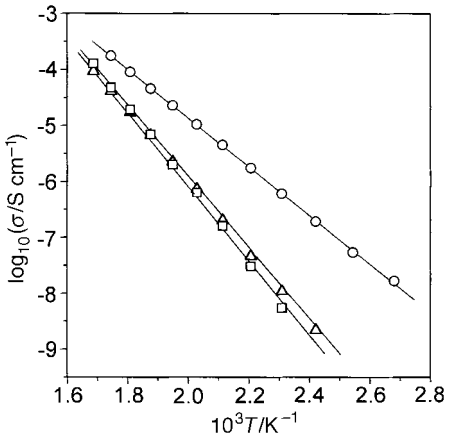

Fig. 5 Ionic conductivity *vs.* inverse temperature in an Arrhenius plot. Circles, triangles and squares correspond to $NaGa(CrO_4)_2$, $KGa(CrO_4)_2$ and $RbGa(CrO_4)_2$, respectively.

in Table 6. The activation energy is lower for the Na compound than the other two, while its ionic conductivity is higher.

Regarding the structure, the distance O2 … O2, between oxygens belonging to two adjacent layers, is the shortest non-bonding distance and, hence, it can operate as a bottleneck in the motion of the alkali ion in the interlayer space. The alkali metal ions diameter (τ),[23] the O2 … O2 distance (d) and the ratio d/r are compared in Table 7. This ratio is higher for $NaGa(CrO_4)_2$ than for $KGa(CrO_4)_2$ and $RbGa(CrO_4)_2$, the ratio being quite similar for the two latter phases. The higher value for the Na compound points to lower hindrance for the motion of Na^+ ions as compared with K^+ and Rb^+ ions. This fact would account for the trend found for the activation energy of the three compounds.

References

1 K. A. Wilhelmi, *Ark. Kemi*, 1966, **261**, 131.
2 J. J. Foster and A. N. Hambly, *Aust. J. Chem.*, 1976, **29**, 2137.
3 K. Brandt, *Ark. Kemi A*, 1943, **17**, 1.
4 F. W Lytle, *Acta Crystallogr.*, 1967, **22**, 321.
5 M. Touboul and P. Popot, *Rev. Chim. Miner.*, 1985, **22**, 610.
6 M. J. Isasi, R. Saez-Puche, M. L. Veiga, C. Pico and A. Jerez, *Mater. Res. Bull.*, 1988, **23**, 395.
7 M. Touboul, S. Denis and L. Seguin, *Eur. J. Solid State Inorg. Chem.*, 1995, **32**, 577.
8 K. A. Wilhelmi, *Acta Chem. Scand.*, 1958, **12**, 6.
9 A. Bonnin, Thesis, Rennes, 1970.
10 Y. Cudennec, Thesis, Rennes, 1978.
11 K. A. Wilhelmi, *Ark. Kemi*, 1966, **26**, 141.
12 A. Hardy and Y. Gabariand, *Acta Crystallogr., Sect. B*, 1978, **28**, 2329.
13 E. J. Graeber and A. Rosenzweig, *Am. Mineral.*, 1971, **56**, 1917.
14 J. W. Anthony and W. John Mc Lean, *Am. Mineral.*, 1972, **57**, 1546.
15 S. Oyetaola, A. Verbgere, Y. Piffard and M. Tournoux, *Eur. J. Solid State Chem.*, 1988, **8**, 259.
16 K. H. Lii, C. C. Wang, R. K. Chang and J. L. Wang, *J. Solid State Chem.*, 1989, **80**, 144.
17 H. M. Rietveld, *Acta Crystallogr.*, 1967, **22**, 151.
18 H. M. Rietveld, *J. Appl. Crystallogr.*, 1969, **2**, 65.
19 J. Rodríguez-Carvajal, in *Abstracts of the Satellite Meeting on Powder Difraction of the XVth. Congress of the International Union of Crystallography,* Tolouse, 1990, p. 127.
20 P. B. Macedo, C. T. Moynihan and R. Bose, *Phys. Chem. Glasses*, 1972, **13**, 171.
21 Y. Hodge, M. D. Ingram and A. R. West, *Electroanal. Chem.*, 1976, **74**, 125.
22 A. Doi, *Solid State Ionics*, 1988, **31**, 227.
23 R. D. Shannon, *Acta Crystallogr., Sect. A*, 1976, **32**, 751.

Paper 8/02707B; *Received* 9*th April*, 1998